

# Extreme oxatriquinanes and a record C–O bond length

Gorkem Gunbas<sup>1</sup>, Nema Hafezi<sup>1</sup>, William L. Sheppard<sup>1</sup>, Marilyn M. Olmstead<sup>1</sup>, Iridi V. Stoyanova<sup>2</sup>, Fook S. Tham<sup>2</sup>, Matthew P. Meyer<sup>3</sup> and Mark Mascala<sup>1\*</sup>

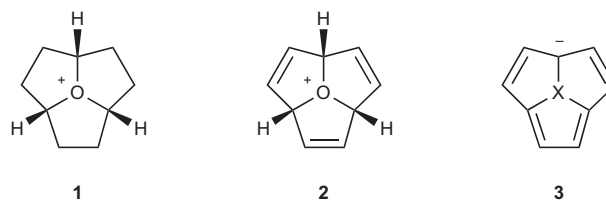
**Oxatriquinanes are fused, tricyclic oxonium ions that are known to have exceptional stability compared to simple alkyl oxonium salts. C–O bonds in ethers are generally  $\sim 1.43$  Å in length, but oxatriquinane has been found to have C–O bond lengths of 1.54 Å. A search of the Cambridge Structural Database turned up no bona fide C–O bond length exceeding this value. Computational modelling of oxatriquinane alongside other alkyl oxonium ions indicated that the electronic consequences of molecular strain were primarily responsible for the observed bond elongation. We also show that substitution of the oxatriquinane ring system with alkyl groups of increasing steric demand pushes the C–O bond to unheard of distances, culminating in a *tert*-butyl derivative at a predicted 1.60 Å. Chemical synthesis and an X-ray crystallographic study of these compounds validated the results of the modelling work and, finally, an extraordinary 1.622 Å C–O bond was observed in 1,4,7-tri-*tert*-butyloxatriquinane.**

Bond lengths, angles and dihedrals are the essential correlations used to interpret collections of atoms as molecules. As such, they are native to the fabric of the natural world and demonstrate a characteristic regularity in their values, with vibrational transitions that occupy pronounced minima on potential energy surfaces. For bonds, any significant compression or elongation away from the equilibrium value incurs considerable energy penalties. This is exemplified in the modelling of diethyl ether, which has an MP2/6-31 + G\*\* calculated C–O bond length of 1.425 Å (refs 1–4). Figure 1a shows that changing this value by  $\pm 15\%$ , to C–O distances unheard of even in the most strained of molecules (1.21 and 1.64 Å), increases the overall energy by 24.7 and 10.3 kcal mol<sup>-1</sup>, respectively. On the other hand, scissoring the C–O–C bond angle  $\pm 15\%$  costs between 5.4 and 9.0 kcal mol<sup>-1</sup> depending on whether the angle is being opened up or squeezed, while a 15% dihedral torsion involves negligible energy costs. This is of course reflected in the force constants of these vibrational modes, which can be determined experimentally or by calculation of the second derivatives of energy with respect to atomic displacement in geometry-optimized structures.

Extremes of bond length or angle values in ground-state molecules, when they are observed, are treated as theoretical curiosities, and may give important insights into the nature of chemical bonding and the relationship (or balance) between the fundamental concepts of steric repulsion (a Pauli exclusion violation)<sup>5</sup> and favourable orbital overlap (termed covalency)<sup>6</sup>. Most literature reports of unusual bond lengths have involved C–C bonds. The mean length of an *sp*<sup>3</sup>C–*sp*<sup>3</sup>C bond, in the absence of branching, is 1.52 Å (ref. 7). Accounts of C–C bonds elongated as a consequence of electronic and/or steric influences have been the subject of reviews<sup>8,9</sup>. The current record holder for a C–C bond in a saturated system is that between the ‘molecular diamond’<sup>10</sup> moieties of diamantyltetramantane<sup>11</sup>. Allowing for unconventional bond definitions pushes this limit even further<sup>12</sup>.

Anomalies in C–heteroatom bond lengths are less commonly singled out for attention. Unbranched amines and ethers have

mean C–N and C–O bond lengths of 1.46 and 1.43 Å, respectively, and searching the primary literature turns up few claims of noteworthy departures from these values, presumably due to the fact that, unlike C–C bonds, stressed C–heteroatom bonds are prone to  $\beta$ -elimination. We first became interested in this subject when we prepared the cyclic oxonium species oxatriquinane (OTQ) **1** and oxatriquinacene **2** in the context of a research programme aimed at the synthesis of heteroacepentalenes **3**, which are formally hemispherical clippings of the corresponding C<sub>20–n</sub>X<sub>n</sub> fullerenes<sup>13</sup>. OTQ **1** was found to have exceptional stability for an alkyl oxonium salt, surviving recrystallization from boiling water and even column chromatography on silica gel, and yet, X-ray crystallography showed that the C–O bond lengths in **1** were remarkably long (1.537 Å)<sup>13</sup>. The C–O bonds of **2**, while not quite as long as those of **1**, still averaged 1.520 Å.



In an attempt to put the C–O bond lengths of **1** into context, we turned to the Cambridge Structural Database (CSD) and searched for structures with C–O bonds  $\geq 1.54$  Å by running a bond distance query in the program CONQUEST<sup>14</sup>. To our surprise, the search returned 5,077 hits, up to a maximum C–O bond length of 2.42 Å. Inspection of the hit set clearly indicated errors. First, over 60% of the long C–O bonds were located in solvent molecules (simple alcohols, ethers and esters), where no credible argument for unusual sterics or electronics could be made. The majority of the remaining hits also involved oxygen in unremarkable contexts, such as crown ethers, carbohydrates and miscellaneous esters.

<sup>1</sup>Department of Chemistry, University of California Davis, 1 Shields Avenue, Davis, California 95616, USA, <sup>2</sup>Department of Chemistry, University of California Riverside, 900 University Avenue, Riverside, California 92521, USA, <sup>3</sup>Department of Chemistry and Biochemistry, University of California Merced, 5200 North Lake Road, Merced, California, 95343, USA. \*e-mail: mjmasca@ucdavis.edu

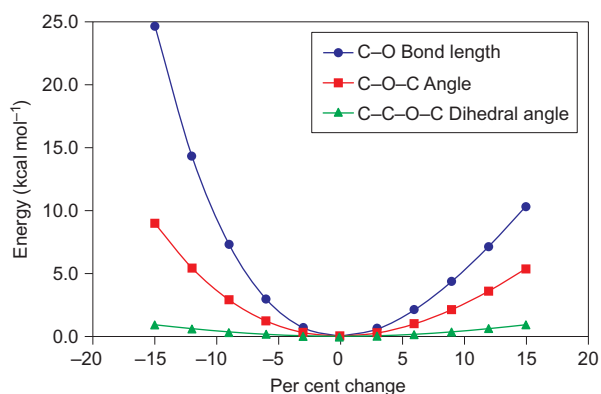


**Figure 1 | Bond length, angle and dihedral distortion energies for diethyl ether (MP2/6-31 + G\*\*).** The limits in the percent changes ( $\pm 15\%$ ) correspond to C–O bond lengths of 1.21 and 1.64 Å, C–O–C angles of 95.3° and 128.9°, and C–O–C–C dihedral angles of 153.0° and 207.0°.

Once these self-evident artefacts were eliminated from consideration, a small number of structures remained for which a case could, in principle at least, be made for an elongation of the C–O bond. After those with disorder within the fragment containing the bond of interest were discarded, ten structures claiming bond lengths of 1.54–1.70 Å were singled out for further examination (see Supplementary page S3 for a list of these structures).

Faced with such a large volume of unreliable crystallographic data, the question becomes how to verify whether a published bond length is bona fide or not. Although analytical methods such as electron diffraction and microwave spectroscopy can be used to experimentally determine gas-phase structures<sup>15</sup>, high-level modelling is now routinely used to corroborate crystallographically measured bond lengths. For example, Schreiner and co-workers determined C–C bond distances of 1.647 Å in a diamondane dimer by X-ray diffraction. This agreed with density functional theory (DFT) calculated values to within 0.001 Å using one functional (M06-2X/6-31G\*\*), although some others performed less well, overestimating the bond lengths by 0.006–0.027 Å (ref. 16). However, given that bond lengths are systematically underestimated in X-ray crystal structures due to libration<sup>17</sup>, it is arguable that the calculations may actually offer a more accurate representation of structures than do the crystallographic data. In our experience, the DFT model of **1** (B3LYP/6-31 + G\*\*) displayed C–O bond distances of 1.535 Å, indicating that the crystal structure was indeed accurate. For the ten hits selected from the original C–O bond length search of the CSD, none had calculated C–O bonds longer than the 1.54 Å originally defined in the search; in fact, only one had a calculated C–O bond length in excess of 1.50 Å. This was an oxonium species obtained by the alkylation of a lactone on the carbonyl oxygen with a Meerwein salt. The crystal structure showed a C–O bond length of 1.538 Å (ref. 18), close to the 1.528 Å we calculated for this system. The authors of this work commented that this was the longest known C–O bond distance<sup>19</sup>, and so it appeared to be, up to then.

Recognizing that the OTQ system was capable of accommodating exceptionally long C–O bonds, we first undertook to examine this bond-lengthening effect in detail, and then to determine to what extent the system could be pushed towards true ‘world record’ C–O bond lengths.

## Results and discussion

The first point to make is that alkyloxonium ions in general have significantly longer C–O bonds than alkyl ethers. Besides **1**, there are seven examples of trialkyloxonium salts in the CSD. The most reliable of these structures (*R*-value of <5%) are trimethyloxonium

hexafluoroarsenate<sup>20</sup>, 1-oxaadamantane 7,8,9,10,11,12-hexachloro-1-carba-closo-dodecaborate<sup>21</sup> and an O-alkylated tetrahydrofuran triflate<sup>22</sup>, the mean C–O bond lengths of which are 1.471, 1.510 and 1.493 Å, respectively. The lengthening of the C–O bonds results from a combination of steric and electronic factors, the nature of which will be discussed here. The same effect is observed in alkyl ammonium salts, but to a lesser extent<sup>23</sup>.

A systematic analysis of C–O bond length trends in increasingly substituted alkyl oxonium species is presented in Table 1, where the variables that influence the bond properties—that is,  $\beta$ -C–H and/or C–C  $\rightarrow \sigma^*(\text{C–O}^+)$  donor–acceptor energies,  $\sigma$ – $\sigma^*$  gap, bond order, bond critical point location, bond electron density and  $\sigma$ -delocalization—provide insights into the structural consequences of increasing substitution in these cations. Starting with the simplest alkyl oxonium ion  $\text{Me}_3\text{O}^+$  (**4**) and building outwards, the progression towards longer C–O bonds generally follows the degree of branching at the  $\alpha$  carbons. The effect of introducing a tetrahydrofuran (THF, **7–10**) or an oxadiquinane ring (**11**, **12**) into the system compresses the intracyclic C–O–C bonds, but the bond length trend is not markedly affected. However, at OTQ **1**, a small but significant increase in C–O bond length over the correspondingly substituted dimethyl oxadiquinane is observed. Adding a single alkyl substituent to the OTQ system (**13**) has the effect of further lengthening the C–O bond at the substituted carbon while slightly contracting the others. The substitution of all three positions with primary (**14**), secondary (**15**) and finally tertiary (**16**) alkyl groups leads to progressively longer C–O bonds, culminating in C–O bond lengths of 1.60 Å in the tri-*tert*-butyl derivative **16**.

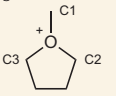
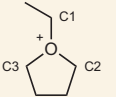
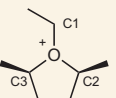
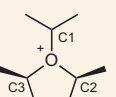
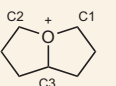
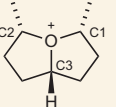
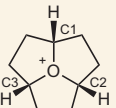
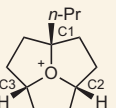
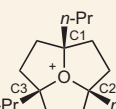
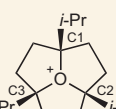
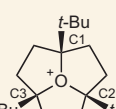
Establishing causality for the greater C–O bond lengths in OTQ structures calls for an analysis of the system’s structure and energetics, which are inextricably linked. Two computational methodologies, natural bond orbital (NBO) analysis and the quantum theory of atoms in molecules (QTAIM), were applied to gain insight into the physical nature of bonding in trialkyloxonium structures<sup>24–26</sup>.

NBO analysis is the repartitioning of numerical valence basis functions into a basis that reflects the conceptual molecular orbital theory framework of organic chemistry. In other words, numerical basis orbitals are repartitioned into  $\sigma$ ,  $\pi$ ,  $\sigma^*$ ,  $\pi^*$  and  $n$  (lone pair) entities. Within the NBO formalism, interactions between filled ( $\sigma$ ,  $\pi$  and  $n$ ) and unfilled ( $\sigma^*$  and  $\pi^*$ ) orbitals can be quantified in terms of an interaction energy (equation (1)). This is important in the trialkyloxonium structures discussed here, because donations into the  $\sigma^*(\text{C–O})$  orbital lengthen the C–O bonds. The numerator in equation (1), which is the square of the Fock operator ( $\hat{F}$ ) matrix element, describes physical overlap between filled ( $\sigma_{\text{filled}}$ ) and empty ( $\sigma_{\text{unfilled}}$ ) orbitals. In general, overlap is maximized between occupied and unoccupied orbitals when they are aligned in an anti-periplanar arrangement. The denominator of equation (1) describes the difference between the energies associated with filled ( $\epsilon_{\text{filled}}$ ) and unfilled ( $\epsilon_{\text{unfilled}}$ ) orbitals. It is important to note that a destabilized C–O bond will have a lower energy associated with its respective antibonding orbital. This feature allows, in general, for more substantial interactions with filled donor orbitals.

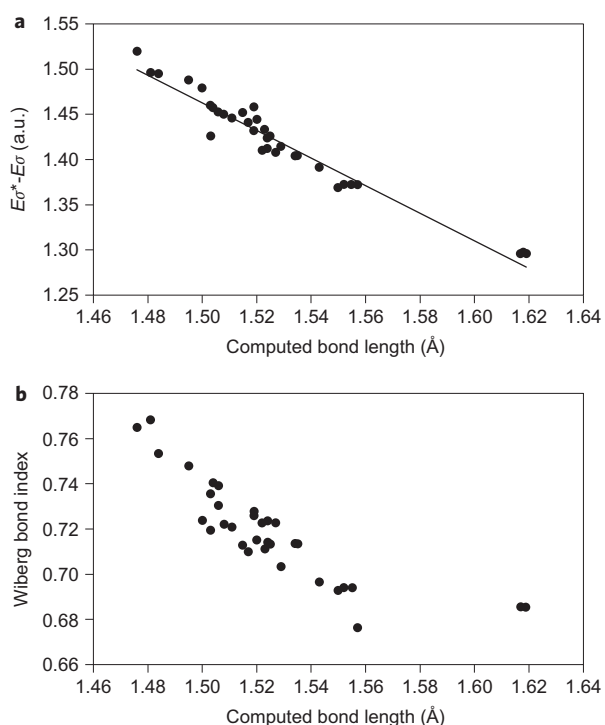
$$\Delta E = 2 \frac{\langle \sigma_{\text{filled}} | \hat{F} | \sigma_{\text{unfilled}} \rangle^2}{\epsilon_{\text{unfilled}} - \epsilon_{\text{filled}}} \quad (1)$$

Figure 2a demonstrates a strong linear correlation between the separation of energies associated with  $\sigma^*(\text{C–O})$  and  $\sigma(\text{C–O})$  orbitals and computed bond lengths in structures **1** and **4–16**. The observed trend is that the gap between antibonding and bonding orbitals decreases as the number of fused rings increases. Ring strain is a plausible explanation for this effect. For comparison, the ring

**Table 1 | Calculated (MP2/6-31 + G\*\*) structural and electronic characteristics of alkyloxonium ions.**

Structure	Bond lengths	$\sum_{\text{donor}} \sigma \rightarrow \sigma^* \text{C-O}^{\ddagger}$	$E\sigma^* - E\sigma^{\ddagger}$	Wiberg bond index	$r_{\text{C-CD}^{\ddagger}}/r_{\text{C-O}^{\text{S}}}$	$\rho^{\parallel}$	$\eta^{\ast}$
$\text{Me}_3\text{O}^+$ (4)	C-O: 1.484	9.24	1.495	0.7534	0.330	0.204	
$\text{Et}_2\text{MeO}^+$ (5)	C1(Me)-O: 1.481 C2(Et)-O: 1.508 C3(Et)-O: 1.511	9.15 19.22 19.91	1.496 1.450 1.446	0.7685 0.7220 0.7210	0.333 0.342 0.343	0.207 0.194 0.193	
$\text{Et}_3\text{O}^+$ (6)	C-O: 1.506	18.44	1.452	0.7304	0.341	0.196	
 7	C1-O: 1.476 C2-O: 1.503 C3-O: 1.518	7.84 16.90 17.00	1.520 1.460 1.432	0.7649 0.7194 0.7279	0.329 0.340 0.348	0.207 0.197 0.191	6.08
 8	C1-O: 1.500 C2-O: 1.503 C3-O: 1.519	18.58 16.15 16.88	1.479 1.426 1.458	0.7239 0.7356 0.7262	0.337 0.342 0.349	0.197 0.198 0.192	6.06
 9	C1-O: 1.495 C2-O: 1.529 C3-O: 1.517	16.95 27.57 26.13	1.488 1.415 1.441	0.7481 0.7035 0.7099	0.340 0.356 0.349	0.199 0.187 0.192	6.07
 10	C1-O: 1.520 C2-O: 1.525 C3-O: 1.524	28.60 27.04 26.90	1.444 1.423 1.424	0.7152 0.7135 0.7142	0.351 0.357 0.352	0.190 0.190 0.191	6.08
 11	C1-O: 1.506 C2-O: 1.504 C3-O: 1.550	16.01 15.28 26.17	1.453 1.457 1.369	0.7391 0.7405 0.6928	0.346 0.346 0.368	0.198 0.199 0.183	6.07
 12	C1-O: 1.523 C2-O: 1.515 C3-O: 1.522	28.20 27.35 21.07	1.433 1.452 1.410	0.7113 0.7130 0.7227	0.353 0.350 0.368	0.188 0.193 0.195	6.07
 1	C1-O: 1.531 C2-O: 1.531 C3-O: 1.531	24.33 24.36 24.34	1.404 1.404 1.404	0.7136 0.7135 0.7135	0.362 0.361 0.361	0.191 0.191 0.191	6.09
 13	C1-O: 1.557 C2-O: 1.524 C3-O: 1.527	34.90 23.16 23.19	1.372 1.412 1.408	0.6764 0.7237 0.7227	0.373 0.361 0.361	0.180 0.193 0.194	6.08
 14	C1-O: 1.543 C2-O: 1.543 C3-O: 1.543	32.49 32.50 32.50	1.391 1.391 1.391	0.6968 0.6968 0.6968	0.371 0.371 0.371	0.186 0.186 0.186	6.07
 15	C1-O: 1.555 C2-O: 1.555 C3-O: 1.555	33.78 33.78 33.78	1.372 1.372 1.372	0.6942 0.6942 0.6942	0.374 0.374 0.374	0.182 0.182 0.182	6.09
 16	C1-O: 1.601 C2-O: 1.602 C3-O: 1.602	37.48 36.69 36.70	1.296 1.297 1.296	0.6856 0.6854 0.6856	0.392 0.392 0.392	0.166 0.166 0.166	6.26

<sup>†</sup>Sum of interaction energies resulting from donations of filled orbitals into unfilled  $\sigma^*(\text{C-O})$  orbitals (in kcal mol<sup>-1</sup>). <sup>‡</sup>Difference between the energies associated with  $\sigma^*(\text{C-O})$  and  $\sigma(\text{C-O})$  bonds (in a.u.). <sup>§</sup>Distance of (3,-1) critical point from the carbon centre expressed as a fraction of the bond length. <sup>||</sup>Electron density at bond critical point in electrons per cubic Bohr radius. <sup>\*</sup> $\sigma$ -delocalization.



**Figure 2 | Trends in C-O distances versus bond attributes.** **a**, Energy separation between antibonding and bonding orbital energies for C-O bonds versus computed C-O bond length in the trialkyloxonium structures in Table 1 [MP2/6-31 + G(d,p)]. **b**, Trend of computed Wiberg bond index versus computed C-O bond length in the trialkyloxonium structures in Table 1 [MP2/6-31 + G(d,p)].

strain associated with cyclopentane, *cis*-[3.3.0]-bicyclooctane and perhydrotriquinacene (carbacycles that are analogous to THF, **11** and **1**) are estimated to be 6.2 (ref. 27), 9.4 (ref. 27) and 15.9 kcal mol<sup>-1</sup> (ref. 28), respectively.

Generally speaking, donations from C-H bonds containing  $\gamma$ -hydrogens are more energetically favourable for C-H bonds residing in acyclic positions than those residing in cyclic structures. This is manifest in comparisons between the summed interaction energies between filled orbitals and individual  $\sigma^*(\text{C-O})$  orbitals for molecules with equivalent degrees of substitution (Table 1). For example, interaction energies in Et<sub>3</sub>O<sup>+</sup> (**6**) are larger than those for  $\sigma^*(\text{C2-O})$  and  $\sigma^*(\text{C3-O})$  in structures **7** and **8** and  $\sigma^*(\text{C1-O})$  and  $\sigma^*(\text{C2-O})$  in **11**. Acyclic substituents are torsionally unconstrained and can donate in an anti-periplanar fashion. In other words, the physical overlap between the largest lobes of the  $\sigma(\text{C-H})$  orbitals and the  $\sigma^*(\text{C-O})$  orbitals is enhanced in acyclic substituents. This increases the value of the Fock operator in the numerator of equation (1). Of course, this tendency would incorrectly predict that **10** should present greater bond lengths than **1**. However, OTQ **1** exhibits a sudden decrease in the separation between the energies associated with  $\sigma(\text{C-O})$  and  $\sigma^*(\text{C-O})$ , which ultimately decreases the denominator of equation (1) and compensates for the imperfect alignment of donor and acceptor orbitals.

Donations from C-H bonds containing  $\gamma$ -hydrogens are generally larger than geometrically analogous donations from C-C bonds. This effect can be attributed to the fact that C-C bonds are energetically more distant from  $\sigma^*(\text{C-O})$  orbitals. The energy levels associated with C-O bonds in **16**, however, are significantly displaced relative to other OTQ species, allowing for effective  $\sigma(\text{C-C})$  donation from the *tert*-butyl substituent into the  $\sigma^*(\text{C-O})$  orbitals. This interaction is worth 8.28 kcal mol<sup>-1</sup> in **16**, whereas a similar interaction in **15** is only worth 6.34 kcal mol<sup>-1</sup>.

QTAIM, developed by Bader<sup>25</sup>, uses electron density to quantitatively define conceptual descriptors that derive from electron density, such as atomic charge and bonding motifs. Among the compounds in Table 1, a trend is evident. The bond critical points move farther away from the carbon atom in the C-O bonds as a function of the degree of substitution. Once again, however, the OTQ series shows a greater displacement of the bond critical points away from the carbon atoms, with structure **16** showing the greatest displacement. Simultaneously, the magnitude of the electron density at the bond critical point ( $\rho$ ) is markedly lower for **16** than for all other trialkyloxonium structures.

Another metric that can be applied to cyclic structures is  $\sigma$ -delocalization,  $\eta$  (ref. 29). This term is the ratio of the average electron density at the five bond critical points over the density at the corresponding ring critical point. This value is essentially constant for all monocyclic, bicyclic and tricyclic structures in Table 1, except **16**, which has a significantly larger degree of  $\sigma$ -delocalization. Taken together, the data from QTAIM analysis suggest that the C-O bond in **16** behaves paradoxically as a more covalent bond than in other trialkyloxonium species. This is also borne out in Fig. 2b, which shows the correlation between Wiberg bond index (a quantitative estimate of bond order that is computed from the sum of overlaps between natural atomic orbitals on the two atoms between which a bond is considered to exist) and calculated bond length<sup>30</sup>. Structure **16** deviates from an otherwise approximately linear relationship, yielding a larger bond index than would be predicted from its bond length.

Thus, the greater C-O bond distances in the OTQ system are rationalized primarily in terms of the development of ring strain in **1** and **13-16**. However, explaining the unique behaviour of *t*-Bu<sub>3</sub>OTQ **16** requires a structural approach. The data clearly suggest an additional role for steric interactions, where some H-H

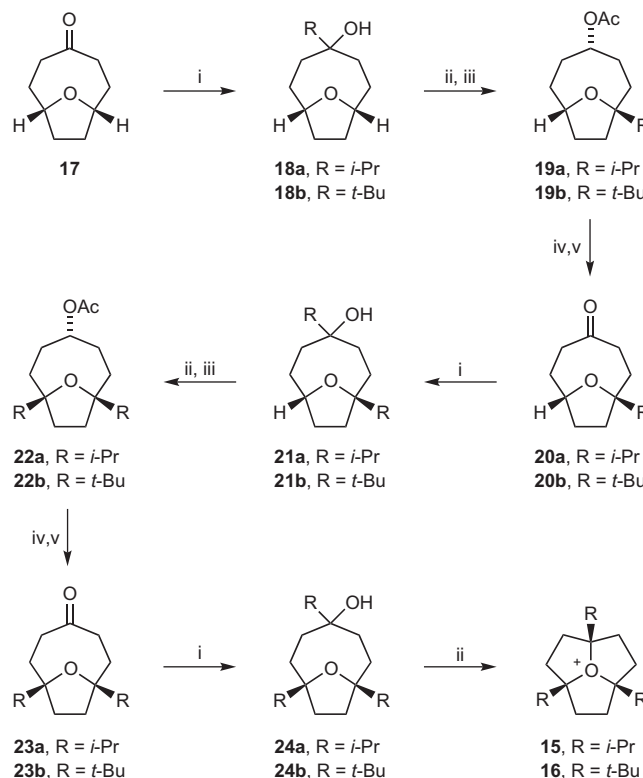


**Figure 3 | Synthesis of substituted oxatriquinanes **15** and **16**.** i, RMgCl, LaCl<sub>3</sub> · 2LiCl or RLi, THF; ii, TfOH, MeCN; iii, NaOAc; iv, K<sub>2</sub>CO<sub>3</sub>, MeOH; v, CrO<sub>3</sub>, pyridine, CH<sub>2</sub>Cl<sub>2</sub>. Overall yields for **17** → **24** (11 steps): 15.8% (**24a**) and 10.4% (**24b**).

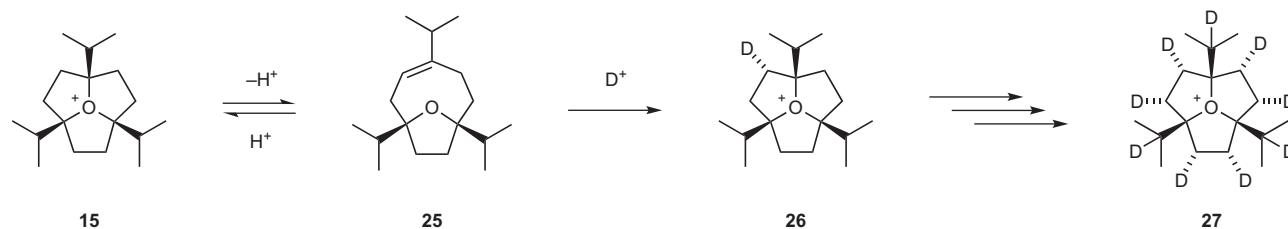


**Figure 4 | Deuterium exchange in 15 in D<sub>3</sub>COD solution.** The *endo* stereochemistry of the deuterium substituents was established by the <sup>1</sup>H-NMR shifts of the residual protons.

distances are less than the sum of the van der Waals radii. QTAIM provides further evidence for a steric interaction in **16**, in that a bond critical point is found between its closest hydrogen atoms. This critical point has significant electron density, with  $\rho = 0.014$ —a value that is comparable to the electron density local to the bond critical point between occluded hydrogen atoms in the transition structure for biphenyl inversion ( $\rho = 0.013$ )<sup>31</sup>. In contrast, bond critical points between the nearest hydrogen atoms in the *iso*-propyl analogue **15** have electron densities of  $\rho = 0.008$ .

Stimulated by the data in Table 1 and the opportunity to realize molecules with unprecedented C–O bond lengths, we set out to structurally characterize OTQs **13**–**16**. The synthesis of PrOTQ **13** and Pr<sub>3</sub>OTQ **14** has been described in a previous work<sup>32</sup>. The synthesis of substituted OTQs **15** and **16** is shown in Fig. 3. Both of these target compounds could be derived from the common bicyclic ketone intermediate **17**, which itself is prepared in eight steps from 1,5-cyclooctadiene<sup>13,33</sup>. Thus, lanthanum-promoted Grignard addition to ketone **17** gives tertiary alcohols **18**, treatment of which with triflic acid produces the mono *i*-Pr- and *t*-Bu-OTQ intermediates, which are not isolated but ring-opened with acetate to give esters **19**. Hydrolysis of the esters and Cr(vi) oxidation provides ketones **20**, which are ready for another round of substitution. Cycling through the Grignard addition, ring closure and acetolysis gives **22**, which is similarly hydrolysed and oxidized to disubstituted ketones **23**. A final Grignard addition in the case of **24a**, or *tert*-butyllithium addition in the case of **24b**, followed by ring closure, gives the target compounds **15** and **16** as the triflate salts.

Tri-*iso*-propyl OTQ **15** triflate was converted into the more soluble PF<sub>6</sub><sup>−</sup> salt by simple anion exchange with an aqueous solution of KPF<sub>6</sub>. Unlike OTQ **1**, cation **15** showed evidence of gradual decomposition in dilute solutions of alcohols at room temperature. An NMR-based experiment to test the stability of **15** in refluxing deuteromethanol led to an interesting insight into its reactivity. After several hours, evidence of exchange of some of the protons for deuterons was seen. This process proceeded to completion within 48 h, and is interpreted mechanistically as shown in Fig. 4. Thus, reversible ring opening to alkene **25** and reprotonation/deuteration leads, at its limit, to **27**.

Tri-*tert*-butyl OTQ **16** had a half-life of only minutes at room temperature, decomposing into a mixture of elimination products and other unidentified materials. It was, however, sufficiently

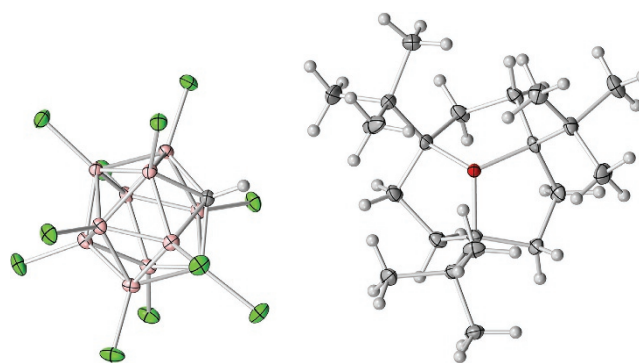


**Figure 5 | X-ray crystal structure of tri-*tert*-butyl oxatriquinane **16** and its [CHB<sub>11</sub>Cl<sub>11</sub>]<sup>−</sup> counterion.** Atom colours: grey, C; white, H; red, O; pink, B; green, Cl.

stable to allow collection of <sup>1</sup>H- and <sup>13</sup>C-NMR data, which showed an averaged C<sub>3v</sub> symmetry.

Crystallization of salts **13**–**15** for X-ray diffraction analysis proceeded uneventfully. However, because of the marginal stability of tri-*tert*-butyl OTQ **16**, an alternative approach had to be taken. Instead of closing down the precursor alcohol with acid, it was dehydrated to the corresponding alkene and then treated with the benzenium acid [C<sub>6</sub>H<sub>7</sub>]<sup>+</sup> [CHB<sub>11</sub>Cl<sub>11</sub>]<sup>−</sup>. X-ray quality crystals of **16** [CHB<sub>11</sub>Cl<sub>11</sub>]<sup>−</sup> could be grown from CH<sub>2</sub>Cl<sub>2</sub> at −40 °C. All of the structures **13**–**16** were of good accuracy, with *R*-values of <5%.

The structural data for the OTQs is given in Table 2. The previously described OTQ **1** structure establishes a baseline for this system at a C–O distance of 1.537 Å. Consistent with modelling, the effect of monosubstitution of OTQ is that the bond between the oxygen and the tertiary carbon in **13** lengthens (1.548 Å), while the other two C–O bonds contract (1.525, 1.528 Å). Tri-*n*-propyl substitution, as in **14**, results in a lengthening of all three C–O bonds relative to **1**, with an average C–O distance of 1.554 Å. Virtually no change is seen in the transition from the primary alkyl substituents in **14** to secondary alkyl substituents in **15** (1.556 Å). However, the tertiary alkyl groups of **16** clearly exert a strong effect on the system, where C–O bond lengths between 1.591 and 1.622 Å are observed. This latter value appears to be the longest accurately measured C–O bond to date. The X-ray crystal structure of **16** is shown in Fig. 5.

## Conclusions

Extremes in chemical bonding are of interest first as theoretical curiosities, but also within the context of understanding the limits of covalency and the consequences of molecular strain. In this study, the remarkable stability of the fused tricyclic OTQ system enabled the observation of otherwise implausible C–O bond distances. Computational modelling is shown to be a valuable resource for challenging literature claims of extraordinary bond lengths, confirming bona fide cases of bonding extremes, and as a means to deconvolute the subtle electronic influences that lead to anomalous

**Table 2 | Experimental and calculated C–O bond lengths in substituted oxatriquinanes.**

Structure	Calculated <sup>†</sup> C–O bond lengths (Å)	Experimental C–O bond lengths (Å)
OTQ ( <b>1</b> )	1.531	1.537
PrOTQ ( <b>13</b> )	1.524, 1.527, 1.557	1.525, 1.528, 1.548
Pr <sub>3</sub> OTQ ( <b>14</b> )	1.543	1.550, 1.554, 1.558
<i>i</i> -Pr <sub>3</sub> OTQ ( <b>15</b> )	1.555	1.556
<i>t</i> -Bu <sub>3</sub> OTQ ( <b>16</b> )	1.601, 1.602, 1.602	1.591, 1.593, 1.622

<sup>†</sup>MP2/6-31+G(d,p)

bonding outcomes. Four substituted OTQs (13–16) were predicted by modelling to have even longer C–O bond distances than the 1.54 Å C–O bonds in **1**, culminating in 1,4,7-tri-*tert*-butyloxatriquinane **16** at a C–O bond length of 1.60 Å. Synthesis and crystal structure determinations verified the results of the computational study and, in the end, a 1.622 Å C–O bond was observed in **16**. We look forward to further exploiting the heterotriquinane molecular framework to investigate C–heteroatom bonds in other unusual contexts, including hypervalency and as ‘frozen’ intermediates on reaction landscapes. Work along these lines is under way and will be reported in due course.

Received 14 June 2012; accepted 16 October 2012;  
published online 18 November 2012

## References

- Møller, C. & Plesset, M. S. Note on an approximation treatment for many-electron systems. *Phys. Rev.* **46**, 618–622 (1934).
- Ditchfield, R., Hehre, W. J. & Pople, J. A. Self-consistent molecular-orbital methods. IX. An extended Gaussian-type basis for molecular-orbital studies of organic molecules. *J. Chem. Phys.* **54**, 724–728 (1971).
- Hehre, W. J., Ditchfield, R. & Pople, J. A. Self-consistent molecular orbital methods. XII. Further extensions of Gaussian-type basis sets for use in molecular orbital studies of organic molecules. *J. Chem. Phys.* **56**, 2257–2261 (1972).
- Hariharan, P. C. & Pople, J. A. The influence of polarization functions on molecular orbital hydrogenation energies. *Theor. Chim. Acta* **28**, 213–222 (1973).
- Weinhold, F. & Landis, C. R. *Valency and Bonding: A Natural Bond Orbital Donor–Acceptor Perspective* (Cambridge Univ. Press, 2005).
- Hoffmann, R. & Hopf, H. Learning from molecules in distress. *Angew. Chem. Int. Ed.* **47**, 4474–4481 (2008).
- Allen, F. H. *et al.* Tables of bond lengths determined by X-ray and neutron-diffraction. 1. Bond lengths in organic compounds. *J. Chem. Soc. Perkin Trans. 2*, S1–S19 (1987).
- Kaupp, G. & Boy, J. Overlong C–C single bonds. *Angew. Chem. Int. Ed. Engl.* **36**, 48–49 (1997).
- Chandrasekhar, J. Organic structures with remarkable carbon carbon distances. *Curr. Sci.* **63**, 114–116 (1992).
- Dahl, J. E., Liu, S. G. & Carlson, R. M. K. Isolation and structure of higher diamondoids, nanometer-sized diamond molecules. *Science* **299**, 96–99 (2002).
- Fokin, A. A. *et al.* Stable alkanes containing very long carbon–carbon bonds. *J. Am. Chem. Soc.* **134**, 13641–13650 (2012).
- Oliva, J. M., Allan, N. L., Schleyer, P. V., Vinas, C. & Teixidor, F. Strikingly long C–C distances in 1,2-disubstituted ortho-carboranes and their dianions. *J. Am. Chem. Soc.* **127**, 13538–13547 (2005).
- Mascal, M., Hafezi, N., Meher, N. K. & Fettingner, J. C. Oxatriquinane and oxatriquinacene: extraordinary oxonium ions. *J. Am. Chem. Soc.* **130**, 13532–13533 (2008).
- Bruno, I. J. *et al.* New software for searching the Cambridge Structural Database and visualising crystal structures. *Acta Crystallogr.* **B58**, 389–397 (2002).
- Spiridonov, V. P., Vogt, N. & Vogt, J. Determination of molecular structure in terms of potential energy functions from gas-phase electron diffraction supplemented by other experimental and computational data. *Struct. Chem.* **12**, 349–376 (2001).
- Schreiner, P. R. *et al.* Overcoming lability of extremely long alkane carbon–carbon bonds through dispersion forces. *Nature* **477**, 308–311 (2011).
- Jones, P. G. Crystal structure determination: a critical view. *Chem. Soc. Rev.* **13**, 157–172 (1984).
- Childs, R. F., Kostyk, M. D., Lock, C. J. L. & Mahendran, M. Structural studies on 6-ethoxytetrahydropyrylium cations; stereoelectronic control in the reactions of lactonium salts. *Can. J. Chem.* **69**, 2024–2032 (1991).
- Childs, R. F. *et al.* Structure, energetics and homoaromaticity. *Pure Appl. Chem.* **58**, 111–128 (1986).
- Lork, E., Görtler, B., Knapp, C. & Mews, R. Alkylation of OPF<sub>3</sub> by MeOSO<sup>+</sup>AsF<sub>6</sub><sup>−</sup>: the unexpected formation of a dioxadiarsetane. *Solid State Sci.* **4**, 1403–1411 (2002).
- Etzkorn, M. *et al.* 1-Oxonoadamantane. *Eur. J. Org. Chem.* 4555–4558 (2008).
- Akkerman, K., Beckmann, J. & Duthie, A. 1,1′-(1,4-Butanediyl)-bis(tetrahydrofuranium) trifluoromethanesulfonate. *Acta Crystallogr.* **E62**, o2781–o2782 (2006).
- Ishida, H. Protonation effect on C–N bond length of alkylamines studied by molecular orbital calculations. *Z. Naturforsch.* **55a**, 769–771 (2000).
- Reed, A. E., Curtiss, L. A. & Weinhold, F. Intermolecular interactions from a natural bond orbital, donor–acceptor viewpoint. *Chem. Rev.* **88**, 899–926 (1988).
- Bader, R. F. W. Atoms in molecules. *Acc. Chem. Res.* **18**, 9–15 (1985).
- Bader, R. F. W. A quantum theory of molecular structure and its applications. *Chem. Rev.* **91**, 893–928 (1991).
- Wiberg, K. B. Concept of strain in organic chemistry. *Angew. Chem. Int. Ed. Engl.* **25**, 312–322 (1986).
- Engler, E. M., Andose, J. D. & von Schleyer, P. R. Critical evaluation of molecular mechanics. *J. Am. Chem. Soc.* **95**, 8005–8025 (1973).
- Cremer, D. & Kraka, E. Theoretical determination of molecular structure and conformation. 15. Three-membered rings: bent bonds, ring strain, and surface delocalization. *J. Am. Chem. Soc.* **107**, 3800–3810 (1985).
- Wiberg, K. A. Application of the Pople–Santry–Segal CNDO method to the cyclopropylcarbinyl and cyclobutyl cation and to bicyclobutane. *Tetrahedron* **24**, 1083–1096 (1966).
- Cioslowski, J. & Mixon, S. T. Topological properties of electron density in search of steric interactions in molecules: electronic structure calculations on ortho-substituted biphenyls. *J. Am. Chem. Soc.* **114**, 4382–4387 (1992).
- Stoyanov, E. S. *et al.* The R<sub>3</sub>O<sup>+</sup>⋯H<sup>+</sup> hydrogen bond: toward a tetracoordinate oxadionium(2+) ion. *J. Am. Chem. Soc.* **134**, 707–714 (2012).
- Mascal, M., Hafezi, N. & Toney, M. D. 1,4,7-Trimethyloxatriquinane: S<sub>N</sub>2 reaction at tertiary carbon. *J. Am. Chem. Soc.* **132**, 10662–10664 (2010).

## Acknowledgements

This work was supported financially by the National Science Foundation (grants CHE-0957798 to M.M. and CHE-1058483 to M.P.M.). G.G. thanks the Turkish Higher Education Council for a studentship.

## Author contributions

G.G. performed synthetic, computational and crystallographic work. N.H. and W.L.S. performed synthetic work. M.M.O. provided assistance with crystallographic work. I.V.S. obtained crystals of **16**. F.S.T. performed the crystallographic work on **16**. M.P.M. performed computational work and interpreted computational results. M.M. supervised the project, composed the manuscript, and performed database and computational work.

## Additional information

Supplementary information and chemical compound information are available in the online version of the paper. Reprints and permission information is available online at <http://www.nature.com/reprints>. Correspondence and requests for materials should be addressed to M.M.

## Competing financial interests

The authors declare no competing financial interests.